Multi-scale Modelling of Iron Impurity in Photovoltaic Devices

Oras A. Al-Ani*, J. P. Goss, Ahmed M.A. Sabaawi, P. R. Briddon, M. J. Rayson and N. E. B. Cowern
School of Electrical and Electronic Engineering, Newcastle University, Merz Court, NE1 7RU, Newcastle upon Tyne, UK.
*o.a.s.al-ani@newcastle.ac.uk

❖ Introduction

In silicon solar cell devices, bulk distortion that may be caused by extended defects (EDs) such as intrinsic stacking faults (ISF) and grain boundaries (GBs) has considerable effects on the physical properties of photovoltaic bulk material [1]. However, at the extremum of disorder, these structural imperfections are known to have a beneficially increased or decreased band gap [2] and absorption coefficient depending on the strain degree that caused by these EDs, as well as their roles to segregate and interact with diffusing impurities such as iron.

❖ Aim

To model the energies and structures of interstitial Fe (with different concentration) in bulk silicon and in the vicinity of ISFs and ∑5 (001) twist GBs in order to predict their effects on solar energy performance.

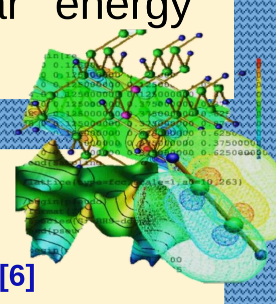

❖ Simulation methods

1) Density functional Theory: AIMPRO [6]

- Dielectric function: Complex, energy dependent Ref. index.
- Computational convergence of image part of Refractive index:
  - ❖ All occupied bands
  - ❖ Around 3 times as many empty bands
  - ❖ Dense sampling scheme to integrate over the Brillion zone.

ED	Sampling	Energy Densities (mJ/m²)		
		Present work	Previous theory	Experiment
ISF	4×4×2	40	26-40 [4]	44 [5]
GB	Γ	1289	1288 [6]	942 [7]

2) TCAD Sentaurus [7]

▪ Processes:
- ❖ Generation via the transfer matrix rate
- ❖ Recombination via Shockly-Read-Hall recombination rate.

▪ Solar cell parameter:
- ❖ Short-cct. current-density (J_{sc})
- ❖ Open-cct. voltage (V_{oc})
- ❖ Device efficiency (η%)

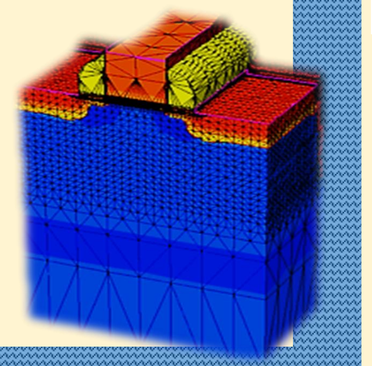

❖ Reference

[1] T. A. Arias and J. D. Joannopoulos, Phys. Rev. B, vol. 49, no. 7, p. 4525, 1994.
[2] R. Raghunathan, et al., Nano Letters, vol. 14, no. 9, pp. 4943–4950, 2014.
[3] M. Chou, et al. , Phys. Rev. B, vol. 32, p.7979, 1985.
[4] M. Chou, et al. , Phys. Rev. B, vol. 32, p.7979, 1985.
[5] S. Altmann, et al., J. Phys. C, vol. 15, p. 5581, 1982.
[6] M. Payne, et al., Phys. Rev. Lett., vol. 58, p. 1348, 1987.
[7] S. Dillon, et al., J. Am. Ceramic Soc., vol.92, p. 1580, 2009.
[8]] Sentaurus TCAD, Version I-2013.12, Synopsys Inc., edition 2013.
[9] G. Masetti, M. Severi, and S. Solmi, vol. 30, no. 7, pp. 764–769, 1983.

❖ Optical Simulation Results

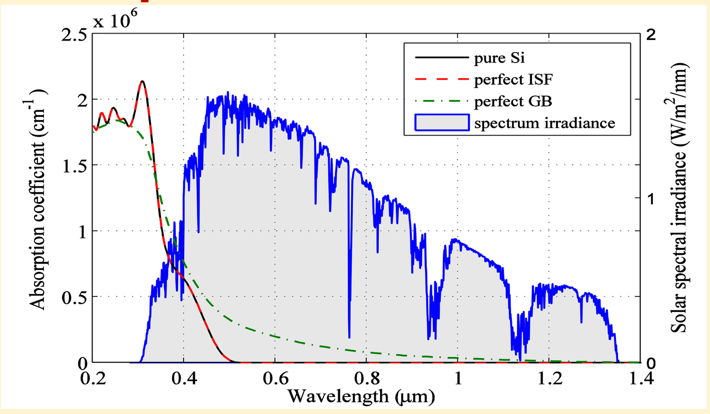

Fig. 2. Calculated optical absorption coefficient versus wavelength for extended defects and ideal Si together with the AM1.5g solar power spectrum for comparison.

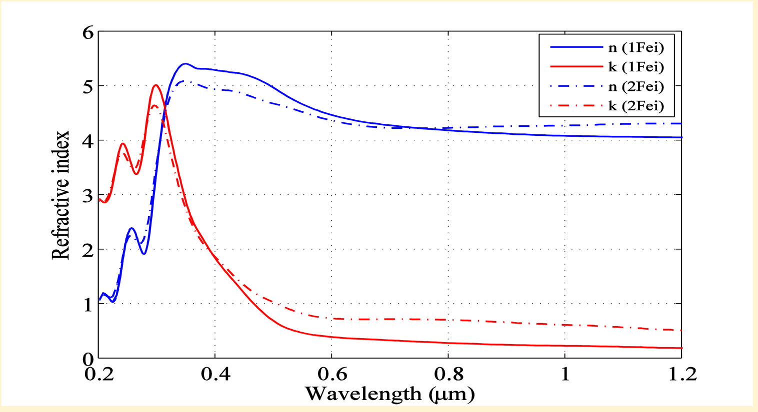

Fig.3. Comparison between the optical properties of the individual iron and iron pair.

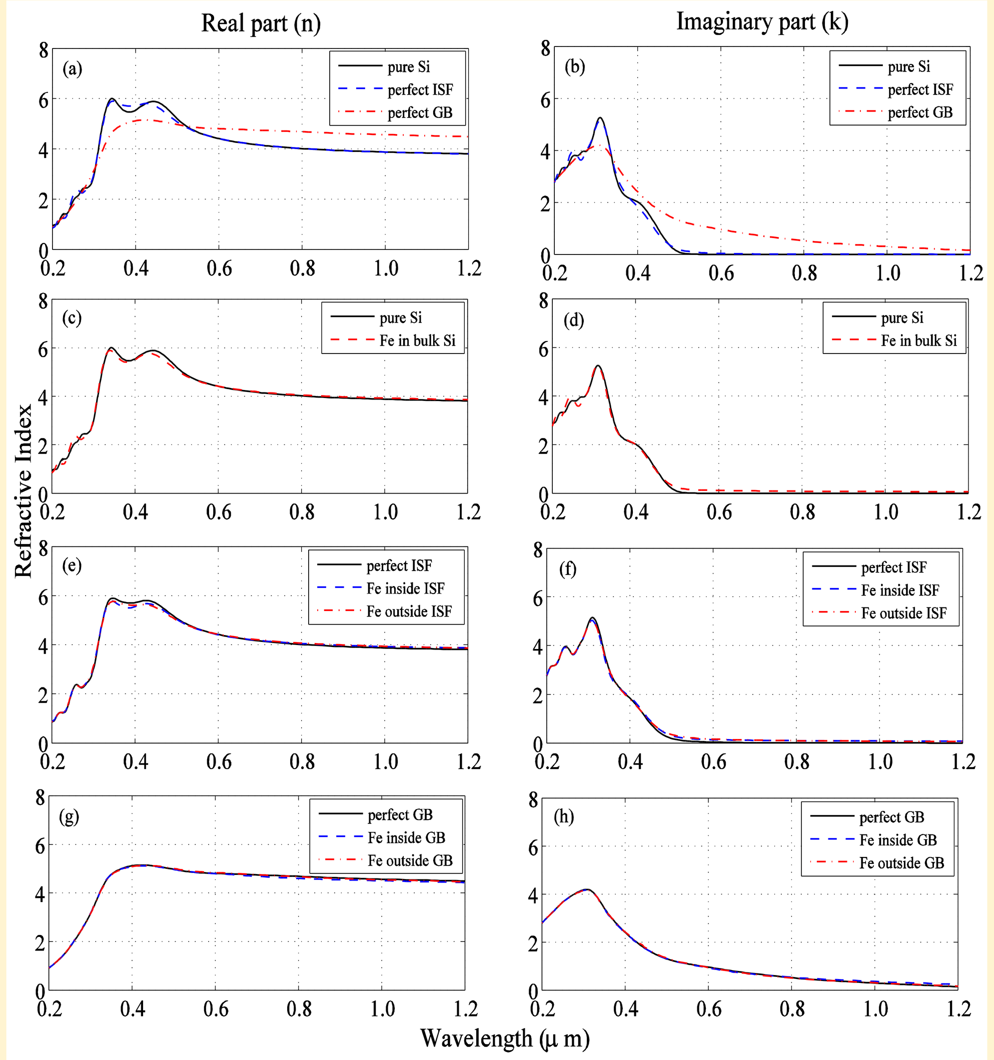

Fig. 4. Computed real (n) and imaginary (k) parts of the refractive index for different structures showing the impact of ED and Fe contamination.

❖ Geometry and Segregation energy

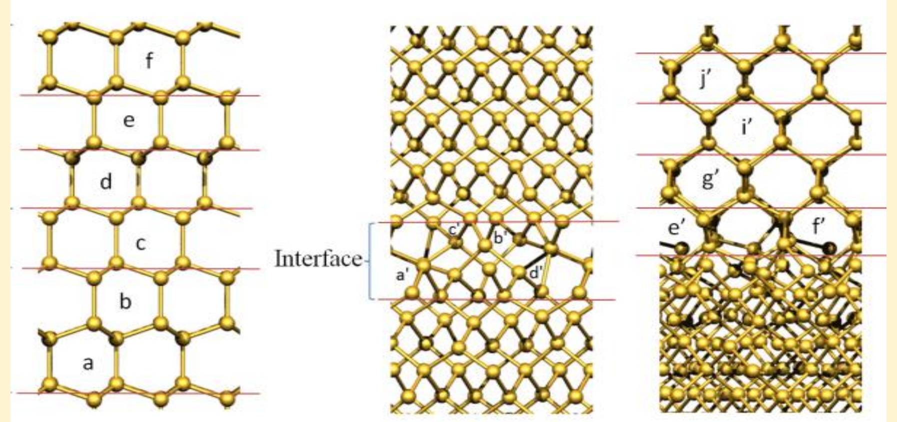

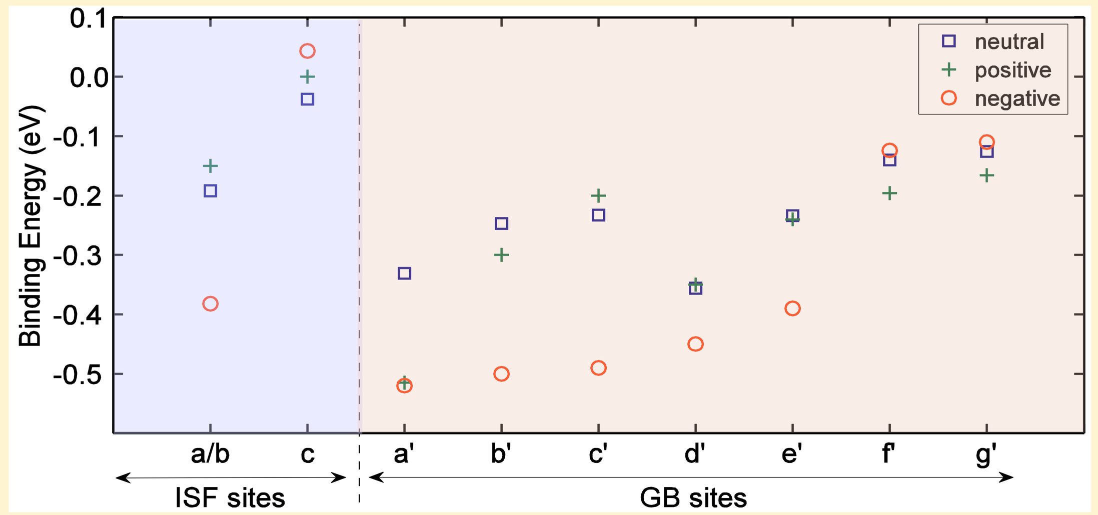

Fig. 1: Binding energy of iron to the ISF and ∑5 GB as a function of site and charge state. In each case, the energies of the lowest energy spin configurations are used. Labels a–f and a′–i′ indicate the non-equivalent interstitial sites investigated

❖ Device Simulation Results

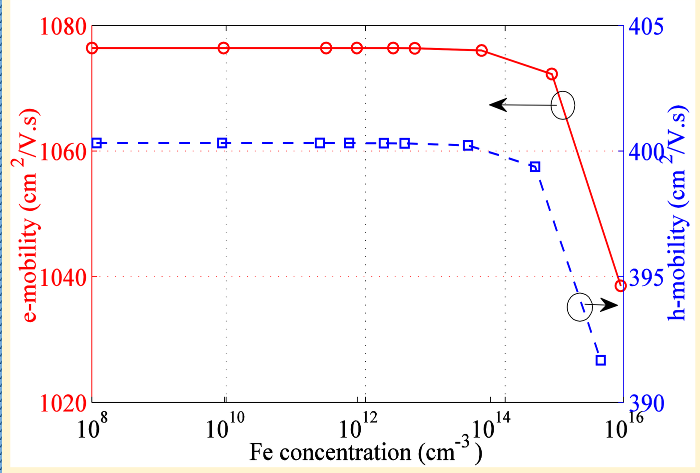

Fig. 5. Variation of carrier mobility with Fe concentration, (left) electron mobility and (right) hole mobility.

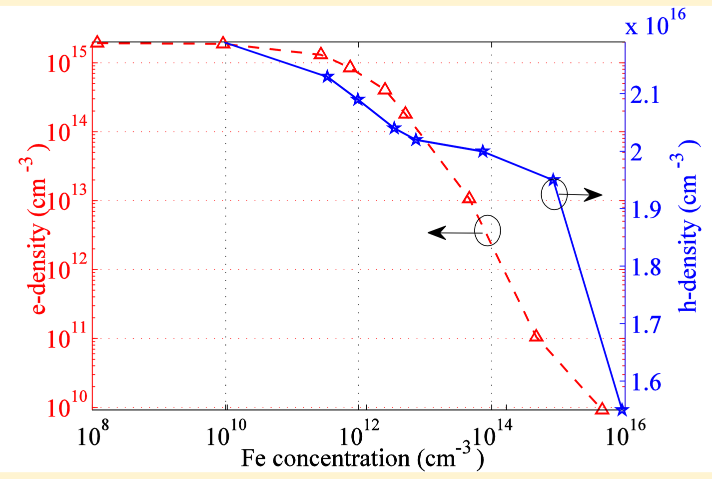

Fig. 6. Variation of carrier density with Fe concentration, (left) electron density and (right) hole density.

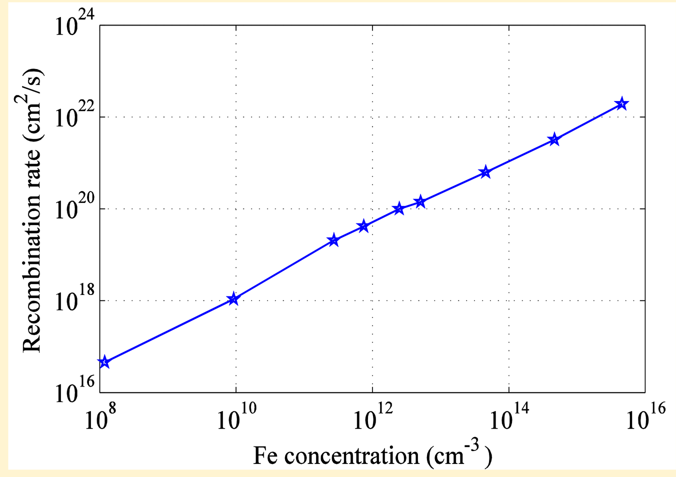

Fig. 7. Variation of recombination rate with increasing impurity oncentration.

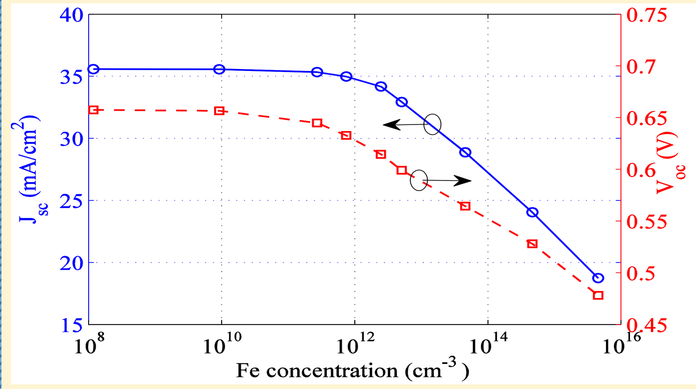

Fig. 8. Current density (left) and open circuit voltage (right) versus impurity concentration.

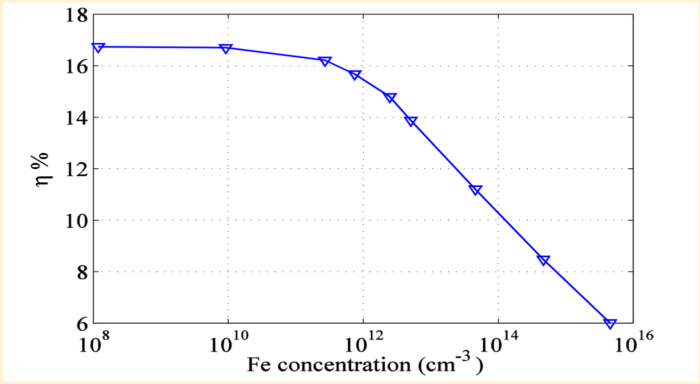

Fig. 9. Conversion efficiency versus Fe impurity concentration.

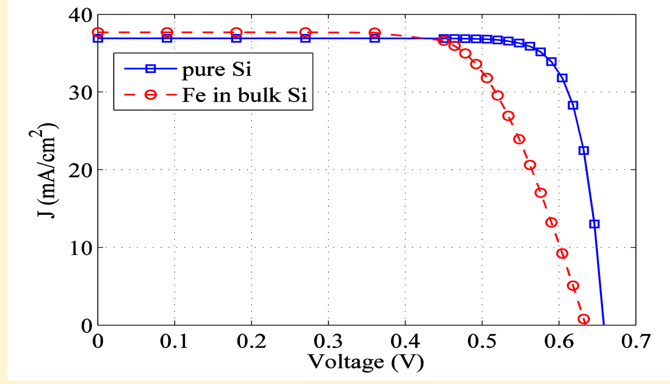

Fig.10 J-V characteristics of silicon solar cell showing the Fe impurity influence.

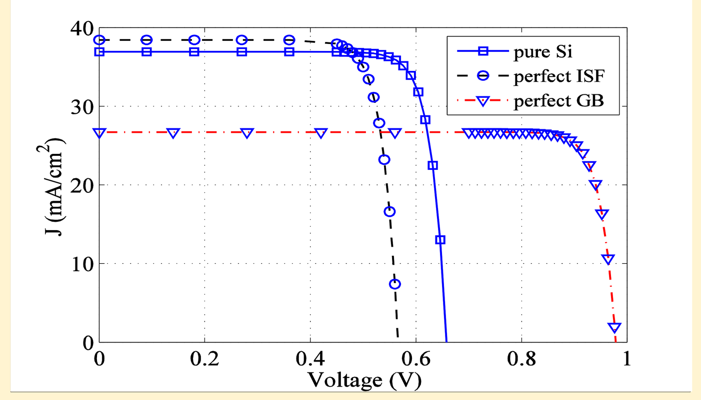

Fig. 11. J-V characteristics of a silicon solar cell with ISF and GB compared with an ideal case.

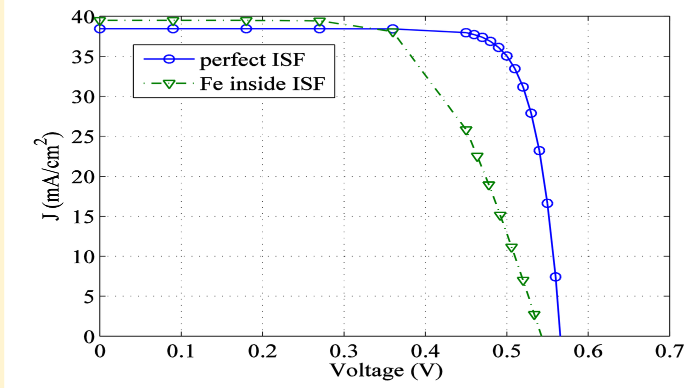

Fig. 12. J-V characteristics of silicon solar cell showing the interaction of ISF with Fe_i impurity.

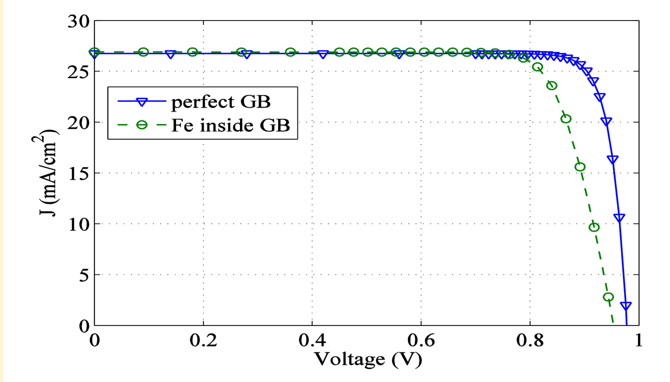

Fig. 13. J-V characteristics of silicon solar cell showing the interaction of GB with Fe_i impurity.

❖ Results summary

Table I: Key results from the solar cell device for pure and perfect EDs under AM 1.5 illumination.

Structure	J_{sc} (mA/cm²)	V_{oc} (V)	FF	η (%)
Ideal Si	36.92	0.65	83.36	20.25
Si with ISF	38.44	0.56	81.29	17.68
Si with GB	26.73	0.67	87.65	22.92

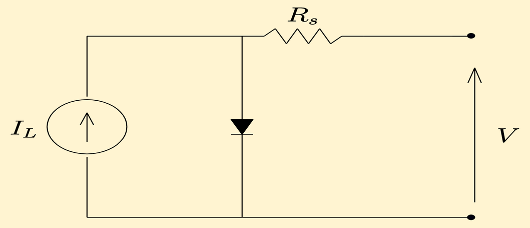

Fig. 14. Parasitic series resistance in a solar cell. circuit. The reduction in FF is modelled as series resistance

Table II: Key results from the solar cell device for pure and doped Si for different Fe concentration under AM 1.5 illumination.

Structure	Fe concentration (cm⁻³)	j_{sc} (mA/cm²)	V_{oc} (V)	FF	η (%)
Pure Si	-	36.92	0.65	83.36	20.25
Individual Fe in bulk Si	1.17 x 10^8	37.71	0.65	70.90	17.62
	7.91 x 10^{11}	37.69	0.63	69.91	16.73
	4.52 x 10^{15}	35.20	0.49	61.99	10.84
Iron pair in bulk Si	1.17 x 10^8	36.82	0.65	71.14	17.24
	7.91 x 10^{11}	36.82	0.63	70.21	16.39
	4.52 x 10^{15}	36.45	0.49	61.78	11.22
Individual Fe in ∑5-(001)	1.17 x 10^8	26.89	0.97	81.41	18.37
	7.91 x 10^{11}	26.89	0.95	80.96	17.53
	4.52 x 10^{15}	26.62	0.81	75.79	11.96
Iron pair in ∑5-(001)	1.17 x 10^8	26.86	0.97	81.42	18.06
	7.91 x 10^{11}	26.86	0.95	80.96	17.24
	4.52 x 10^{15}	26.59	0.81	75.80	12.26

❖ Conclusion

The results show that Fe-impurity has trivial impact on the open-circuit voltage and short-circuit current of solar cell. However, it significantly influence the fill factor, which in turn degrades the conversion efficiency, which is modelled as series resistance.